

Proceedings Article

# Core size analysis of magnetic nanoparticles using frequency mixing magnetic detection with a permanent magnet as an offset source

A. M. Pourshahidi<sup>a,b,\*</sup>, A. Offenhäusser<sup>a,b</sup>, H.-J. Krause<sup>a,c</sup>

<sup>a</sup>Institute of Biological Information Processing, Bioelectronics (IBI-3), Forschungszentrum Jülich, Germany

<sup>b</sup>Faculty of Mathematics, Computer Sci. and Natural Sci., RWTH Aachen University, 52062 Aachen, Germany

<sup>c</sup>Inst. of Nano- and Biotechnologies (INB), FH Aachen University of Applied Sciences, 52428 Jülich, Germany

\*Corresponding author, email: [a.pourshahidi@fz-juelich.de](mailto:a.pourshahidi@fz-juelich.de)

© 2023 Pourshahidi *et al.*; licensee Infinite Science Publishing GmbH

This is an Open Access article distributed under the terms of the Creative Commons Attribution License (<http://creativecommons.org/licenses/by/4.0>), which permits unrestricted use, distribution, and reproduction in any medium, provided the original work is properly cited.

## Abstract

Frequency mixing magnetic detection (FMMD) has been widely used in magnetic immunoassay measurement techniques. It can also be used to characterize and distinguish different magnetic nanoparticle (MNP) types according to their magnetic cores size. In a previous work, a method for resolving ambiguities in determination of the core size distribution was utilized involving measurement of total iron mass. Recently, a new FMMD measurement head was developed in which a pair of permanent ring magnets are used to generate the static offset magnetic field. Here, we show that this new measurement head can be applied for determining the core size distribution of MNP, and compare the results with the outcomes of our conventional electromagnet offset module FMMD.

## 1. Introduction

The usage of magnetic nanoparticle particles (MNPs) in many research fields with biomedical applications has become widespread [1–3]. Various methods are employed for the characterization of the synthesized particles, such as SQUID susceptometry [4], transmission electron microscopy (TEM) [5], dynamic light scattering (DLS) [6] and vibrating sample magnetometry (VSM) [7]. Frequency mixing magnetic detection (FMMD) method has been used as a tool for point of care monitoring (POC) [8,9] as well as analysis of MNP core size distribution [10]. In [11], the ambiguity issue in the determination of the magnetic core sizes of two commercially available MNP types was addressed and resolved using FMMD method in combination with considering the total amount of iron in the sample measured by inductively coupled plasma optical emission spectrometry (ICP-OES). Recently, a

newly developed FMMD measurement head employing a pair of permanent magnets as its static offset magnetic field source, referred to as permanent magnet offset module (PMOM), was introduced in [12]. This new design allows for having a constant temperature throughout the field scans and a reduction in measurement time. However, the static magnetic field cannot be brought down to zero with this setup, the minimum field is 2.6 mT. Here, we report on the application of core size determination using this new system and compare it to the results of our standard electromagnet offset module (EMOM) FMMD.

**Table 1:** Frequency and field setting of the experimental setups.

Setup	$f_1$ [kHz]	$B_1$ [mT]	$f_2$ [Hz]	$B_2$ [mT]
EMOM	40.5	1.29	63	16.4
PMOM	40.5	1.20	63	16.5

**Table 2:** Information on the type of magnetic nanoparticles used.

MNP type	$d_H$ [nm]	Coating	Concentration [mg/ml]
NanomagD Spio	20	Dextran	25

## II. Materials and methods

### II.I. Frequency mixing magnetic detection

The FMMD approach uses a dual-frequency excitation field with a high- and low-frequency,  $f_1$  and  $f_2$ , respectively. When exposed to this dual-frequency excitation field, the ensemble of magnetic nanoparticles yields intermodulations at sum and difference mixing harmonics of the excitation field,  $f_1 \pm n \cdot f_2$ , where  $n$  is an integer number [13].

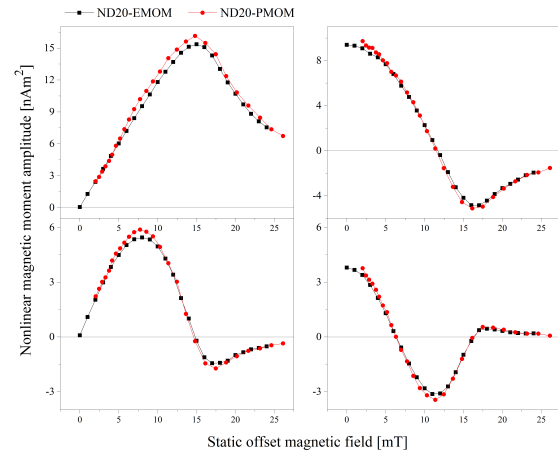
The experimental FMMD setup consists of a magnetic reader synthesizing the dual-frequency excitation signals, and a detection chain including a pre-amplification stage used for the case of digital demodulation using a National Instruments NI-USB 6251 data acquisition card and a PC. In this work, the EMOM setup details of which can be found in [14] and the PMOM setup introduced in [12] were utilized. The operational settings are presented in Table 1.

### II.II. Magnetic nanoparticles

The magnetic nanoparticle type used during this study was procured from Micromod Partikeltechnologie GmbH (Rostock, Germany), see Table 2. The particles are reported to show a lognormal distribution. The sample preparation followed as described in [11] with the final sample concentration of 0.33  $\mu\text{g}/\mu\text{L}$ .

### II.III. Method for core size analysis

The first four static magnetic offset-dependent FMMD signals of the mentioned particles were measured. The results were fitted using the Langevin model of non-interacting particles assuming a lognormal distribution of core sizes with three fitting parameters,  $m(d_0, \sigma, N_p)$ , through a nonlinear least square Levenberg-Marquardt

**Figure 1:** Measured first four nonlinear magnetic moment responses of samples ND20 (NanomagD-Spio  $d_H=20$  nm) with MNP concentration of 0.33  $\mu\text{g}/\mu\text{L}$  at mixing frequencies  $f_1 + f_2$ ,  $f_1 + 2 \cdot f_2$ ,  $f_1 + 3 \cdot f_2$  and  $f_1 + 4 \cdot f_2$  over a static magnetic field range from 0 to 24 mT.

given by

$$f_L(d_c, d_0, \sigma) = \frac{1}{\sqrt{2\pi} \cdot d_c \cdot \sigma} \cdot \exp\left(-\frac{\ln^2(d_c/d_0)}{2\sigma^2}\right) \quad (1)$$

Here,  $d_0$  indicates the median of the distribution and  $\sigma$  the standard deviation of the diameters.

Respectively, the iron mass per sample using the experimental data was calculated through

$$m_{Fe} = \frac{3M_{Fe}}{3M_{Fe} + 4M_O} \cdot \rho_{Fe_3O_4} \cdot N_p \cdot \frac{\pi}{6} \cdot d_0^3 \exp\left(\frac{9\sigma^2}{2}\right) \quad (2)$$

using the molar mass of iron  $M_{Fe} = 55.845$  g/mol and of oxygen,  $M_O = 15.99$  g/mol. Moreover,  $N_p$  denotes the number of particles. Applying a constraint on  $d_0$ , a lookup table for combinations of  $\sigma$  and  $N_p$  yielding an  $R^2 > 0.99$  was created. The total iron mass in the sample was determined using ICP-OES.

## III. Results and Discussion

The measured static offset magnetic field-dependent FMMD signals obtained using both EMOM and PMOM setups are presented in Figure 1. The measurement results for these samples are depicted as solid red circles and solid black squares, respectively.

The look-up graph of the best combinations for the magnetic core distributions leading to  $R^2 > 0.99$  for the fits to the measurements done through both setups are plotted in Figure 2.

The determined core size distribution parameters obtained through the analysis are presented in Table 3. Analysis results yielded  $d_0$  parameter of 13.43 nm for EMOM and 13.80 nm for PMOM.

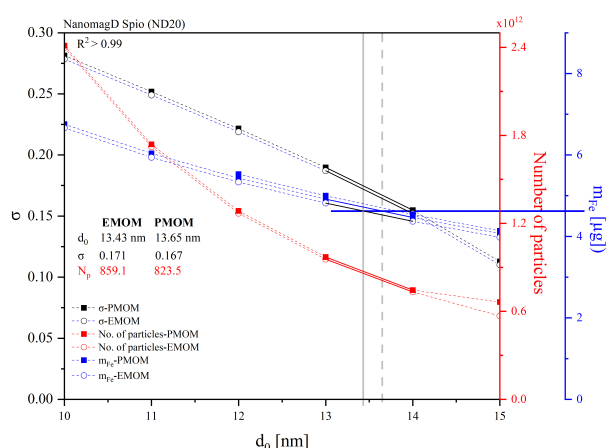


**Figure 2:** Look-up graph of ND20, for the best combinations of the magnetic core size distribution ( $d_0$ ,  $\sigma$ ,  $N_p$ ) leading to  $R^2 > 0.99$ , obtained with both PMOM and EMOM setups.

**Table 3:** Results of lognormal core size distribution parameters obtained with both experimental setups.

Setup	Determined $d_0$ [nm]	Determined $\sigma$
<b>EMOM</b>	13.43	0.171
<b>PMOM</b>	13.80	0.158

The obtained values are very close to each other with a difference of 0.37 nm. In general both values are within the reported range as per the published reports [15,16]. However, deviations to other techniques may arise from the assumption of selected lognormal distribution, errors in measurements and the complex effects of particle-particle interaction. The deviation in the determined values from the two setups may arise from the following points. The effect of the reduced system temperature which has an impact on the amplitude of the measurement signal and the reduced dynamic static field scan range of the PMOM.

## IV. Conclusion

A sample of immobilized magnetic nanoparticles was prepared and measured with the FMMD technique using a standard EMOM and a newly developed PMOM device. The PMOM setup has the advantage that there is no extra heat generated due to the use of a permanent magnet system as the offset magnetic field generating source, hence resulting in reduced overall measurement time because no cool-down time is needed. Core size distribution analysis was performed for the measurement done through both devices. Analysis results yielded  $d_0$  parameter of 13.43 nm for EMOM and 13.80 nm for PMOM measurements. In future, the determined parameters

can be further improved by incorporating the saturation magnetization  $M_s$ .

## Acknowledgments

The authors thank Norbert Wolters for designing and assembling the readout electronics and Dieter Lomparski for construction of the mechanical components and for his assistance in creating the data acquisition software. Research funding from the state of North Rhine-Westphalia and the European Regional Development Fund (ERDF; German: EFRE) under grant number EFRE-0801299, reference number LS-2-1-014c is gratefully acknowledged.

## Author's statement

Conflict of interest: Authors state no conflict of interest.

## References

- [1] Y.T. Chen et al., Biosensing Using Magnetic Particle Detection Techniques, *Sensors* 17, 2300, 2017. doi:10.3390/s17102300.
- [2] K.M. Krishnan, Biomedical Nanomagnetism: A Spin Through Possibilities in Imaging, Diagnostics, and Therapy, *IEEE Trans. Magn.* 46, 2523–2558, 2010. doi:10.1109/TMAG.2010.2046907.
- [3] Q.A. Pankhurst et al. Progress in Applications of Magnetic Nanoparticles in Biomedicine, *J. Phys. D: Appl. Phys.* 42, 224001, 2009. doi:10.1088/0022-3727/42/22/224001.
- [4] D. Hurt et al., Versatile SQUID Susceptometer With Multiple Measurement Modes, *IEEE Trans. Magn.* 49, 3541–3544, 2013. doi:10.1109/TMAG.2013.2241029.
- [5] D. Nieciecka et al., Synthesis and Characterization of Magnetic Drug Carriers Modified with Tb<sup>3+</sup> Ions, *Nanomaterials* 12, 795, 2022. doi:10.3390/nano12050795.
- [6] J. Lim et al., Characterization of Magnetic Nanoparticle by Dynamic Light Scattering, *Nanoscale Res. Lett.* 8, 381, 2013. doi:10.1186/1556-276X-8-381.
- [7] S.E. Sandler et al., Best Practices for Characterization of Magnetic Nanoparticles for Biomedical Applications, *Anal. Chem.* 91, 14159–14169, 2019. doi:10.1021/acs.analchem.9b03518.
- [8] S. Achtsnicht et al., Sensitive and Rapid Detection of Cholera Toxin Subunit B Using Magnetic Frequency Mixing Detection, *PLOS ONE* 14, e0219356, 2019. doi:10.1371/journal.pone.0219356.
- [9] J. Pietschmann et al., Novel Method for Antibiotic Detection in Milk Based on Competitive Magnetic Immunodetection, *Foods* 9, 1773, 2020. doi:10.3390/foods9121773.
- [10] U.M. Engelmann et al., Probing Particle Size Dependency of Frequency Mixing Magnetic Detection with Dynamic Relaxation Simulation, *J. Magn. Magn. Mater.* 563, 169965, 2022. doi:10.1016/j.jmmm.2022.169965.
- [11] A.M. Pourshahidi et al., Resolving Ambiguities in Core Size Determination of Magnetic Nanoparticles from Magnetic Frequency Mixing Data, *J. Magn. Magn. Mater.* 563, 169969, 2022. doi:10.1016/j.jmmm.2022.169969.
- [12] A.M. Pourshahidi et al., Frequency Mixing Magnetic Detection Setup Employing Permanent Ring Magnets as a Static Offset Field Source, *Sensors* 22, 8776, 2022. doi:10.3390/s22228776.

- [13] H.-J. Krause et al., Magnetic Particle Detection by Frequency Mixing for Immunoassay Applications, *J. Magn. Magn. Mater.* 311, 436–444, 2007. doi:10.1016/j.jmmm.2006.10.1164.
- [14] A.M. Pourshahidi et al., Multiplex Detection of Magnetic Beads Using Offset Field Dependent Frequency Mixing Magnetic Detection, *Sensors* 21, 5859, 2021. doi:10.3390/s21175859.
- [15] M. Kallumadil et al., Suitability of Commercial Colloids for Magnetic Hyperthermia. *J. Magn. Magn. Mater.*, 321, 1509–1513, 2009, doi:10.1016/j.jmmm.2009.02.075.
- [16] D. Shahbazi-Gahrouei et al., Superparamagnetic Iron Oxide-C595: Potential MR Imaging Contrast Agents for Ovarian Cancer Detection. *J. Med. Phys.* 38, 198, 2013, doi:10.4103/0971-6203.121198